

## Tumorigenesis and Neoplastic Progression

# Semaphorin 3E Expression Correlates Inversely with Plexin D1 During Tumor Progression

Ilse Roodink,\* Gürsah Kats,\* Léon van Kempen,\*  
Meritha Grunberg,\* Cathy Maass,\* Kiek Verrijp,\*  
Jos Raats,<sup>†‡</sup> and William Leenders\*

From the Department of Pathology,\* Radboud University  
Nijmegen Medical Centre, Nijmegen; ModiQuest Incorporation,<sup>†</sup>  
Nijmegen; and the Department of Biomolecular Chemistry,<sup>‡</sup> Nijmegen  
Centre for Molecular Life Sciences, Nijmegen, The Netherlands

**Plexin D1 (PLXND1) is broadly expressed on tumor vessels and tumor cells in a number of different human tumor types. Little is known, however, about the potential functional contribution of PLXND1 expression to tumor development. Expression of semaphorin 3E (Sema3E), one of the ligands for PLXND1, has previously been correlated with invasive behavior and metastasis, suggesting that the PLXND1-Sema3E interaction may play a role in tumor progression. Here we investigated PLXND1 and Sema3E expression during tumor progression in cases of melanoma. PLXND1 was not expressed by melanocytic cells in either naevi or melanomas *in situ*, whereas expression increased with invasion level, according to Clark's criteria. Furthermore, 89% of the metastatic melanomas examined showed membranous PLXND1-staining of tumor cells. Surprisingly, expression of Sema3E was inversely correlated with tumor progression, with no detectable staining in melanoma metastasis. To functionally assess the effects of Sema3E expression on tumor development, we over-expressed Sema3E in a xenograft model of metastatic melanoma. Sema3E expression dramatically decreased metastatic potential. These results show that PLXND1 expression during tumor development is strongly correlated with both invasive behavior and metastasis, but exclude Sema3E as an activating ligand. (Am J Pathol 2008, 173:1873–1881; DOI: 10.2353/ajpath.2008.080136)**

Cutaneous melanoma is a highly malignant tumor derived from pigment-producing melanocytes in the epidermis. Melanoma frequently develops in a sequence of steps from benign proliferative naevi to atypical naevi, noninvasive *in situ* melanomas (lesions confined to the epidermis), invasive melanomas, and finally to metastases. Clin-

ically, melanomas begin as pigmented lesions that enlarge along an imaginary radius of an imperfect circle, the so-called radial growth phase.<sup>1</sup> At the time of diagnosis many melanomas have progressed to the next phase of progression, or vertical growth phase, which is characterized by invasion of the papillary and reticular dermis.<sup>1</sup> Whereas the relatively indolent radial growth phase melanomas rarely give rise to metastases, vertical growth phase melanomas do have the tendency to metastasize.<sup>2</sup> Furthermore, progression from radial growth phase to vertical growth phase melanoma is accompanied by angiogenesis.<sup>3,4</sup> Stage of disease is usually determined histopathologically by both the maximum vertical tumor thickness (Breslow index) and tumor invasion level (Clark classification).<sup>5</sup>

Many studies have focused on the identification of differentiation markers to distinguish naevi from melanomas. These include mostly nonspecific markers related to cell survival, cell adhesion, and extracellular matrix changes,<sup>6–9</sup> general processes that contribute to tumor growth and metastasis.

Plexins encode large transmembrane proteins that are receptors for neuropilins and semaphorins, a family of secreted or membrane-associated proteins.<sup>10,11</sup> Class 3 semaphorins have been mostly studied in the developing nervous system, where they regulate axonal guidance via activation of plexin/neuropilin complexes.<sup>12–15</sup> The widespread expression of both plexins and semaphorins during embryogenesis, including outside the nervous system, suggests a more general role in physiological and pathological processes.<sup>16,17</sup> We have previously demonstrated that Plexin D1 (PLXND1) is expressed by vascular endothelial cells during developmental angiogenesis.<sup>18</sup> Loss of PLXND1 function in mice and zebrafish leads to lethality due to maldevelopment of the cardiovascular system, indicating a functional role of PLXND1 in vascular patterning.<sup>19,20</sup> Recently, we have shown that PLXND1 is also specifically expressed on vascular endothelium during tumor-associated angiogenesis of primary and met-

---

Supported by the Dutch Cancer Society (grant KUN 2005-3337).

Accepted for publication September 2, 2008.

Address reprint requests to Ilse Roodink, Dept. of Pathology, Radboud University Nijmegen Medical Centre, PO Box 9101, 6500 HB Nijmegen, The Netherlands. E-mail: I.Roodink@pathol.umcn.nl.

astatic tumors, in both animal tumor models and a number of human brain tumors.<sup>21</sup> Interestingly, in the examined metastatic brain tumors, including a melanoma metastasis, we observed abundant specific expression of PLXND1 on tumor cells too.<sup>21</sup> PLXND1 contains in its intracellular domain consensus motifs for Rho-guanine nucleotide exchange factors. Therefore, PLXND1 activation may be predicted to induce cytoskeletal rearrangements, translating into cellular migration and invasion. These processes are fundamental in both angiogenesis and tumor metastasis, suggesting that PLXND1 is functionally involved in tumor development in multiple ways.

Three candidate ligands for PLXND1 have been identified. Semaphorin 3C (Sema3C) binds with high affinity to a Neuropilin-1/PLXND1 complex,<sup>19</sup> whereas binding of semaphorin 3E (Sema3E) or semaphorin 4A (Sema4A) to PLXND1 does not require the presence of neuropilin.<sup>22,23</sup> Interestingly, Sema3E was identified from array analyses as a protein involved in tumor invasion, progression, and metastasis.<sup>24</sup> Collectively, these data suggest an involvement of a PLXND1/Sema3E complex in tumor angiogenesis, tumor cell invasion, and metastasis.

Here we have addressed this hypothesis in two independent ways. First, we analyzed PLXND1 and Sema3E expression by immunohistochemistry on a series of cutaneous melanocytic lesions representing different stages of melanoma progression. Secondly, we examined the effects of overexpression of Sema3E in a melanoma metastasis model. Our results show that PLXND1 expression correlates with tumor invasion level and metastasis in a melanoma progression series. In contrast, Sema3E expression showed a negative association with melanoma progression. This inverse correlation was corroborated in functional studies, which revealed that Sema3E expression, in contrast to Sema3C, resulted in an altered tumor vascular phenotype and significantly reduced metastatic potential.

## Materials and Methods

### Tissue Samples

Formalin-fixed, paraffin-embedded tissue specimens were obtained from the archive of the Department of Pathology of the Radboud University Nijmegen Medical Centre. This study included naevocellular naevi ( $n = 19$ ), dysplastic naevi ( $n = 10$ ), melanomas *in situ* ( $n = 5$ ), primary cutaneous melanomas ( $n = 22$ ), and disseminated melanomas, including skin ( $n = 4$ ), lymph node ( $n = 9$ ), brain ( $n = 5$ ), and lung ( $n = 1$ ) metastases. All primary melanomas were classified by qualified pathologists and graded according to Clark's criteria (II,  $n = 7$ ; III,  $n = 5$ ; IV,  $n = 10$ ) and Breslow thickness.

### Immunohistochemistry

Tissue sections (4  $\mu$ m) were dewaxed and endogenous peroxidase activity was quenched with 3% H<sub>2</sub>O<sub>2</sub> in PBS. Antigen retrieval was performed by digestion with pronase for 9 minutes at 37°C. Subsequently, tissues were pre-incubated with normal horse serum to block nonspe-

cific binding sites, followed by incubation for 1 hour with single domain antibody A12, which was previously selected against a PLXND1-specific peptide.<sup>21</sup> Single domain antibodies were detected by sequential incubations with the mouse monoclonal anti-VSV antibody P5D4, biotinylated anti-mouse IgG (Vector, Burlingame, CA), and avidin-biotin peroxidase complex (Vector) for 1 hour, 30 minutes, and 45 minutes respectively. Peroxidase was visualized by the 3-amino-9-ethylcarbazole (ScyTek, Logan, UT) peroxidase reaction and sections were counterstained with hematoxylin. All incubations were performed at room temperature.

Fifty of the 75 human melanocytic lesions analyzed for PLXND1 expression were immunostained for Sema3E according to standard protocols. In short, antigen retrieval was performed by boiling in 10 mmol/L citrate buffer. Nonspecific binding sites were blocked by incubation with normal horse serum. Slides were incubated overnight at 4°C with goat anti-Sema3E (Abcam Limited, Cambridge, UK), and subsequently detected by sequential incubations with biotinylated anti-goat IgG antibody (Vector) and avidin-biotin peroxidase complex (Vector).

For immunohistochemical analysis of experimental tumors, tissues (tumor, lung) were formalin-fixed and used for (immuno)histological analysis using rat anti-mouse CD34 (Hycult Biotechnology, Uden, The Netherlands), rabbit anti-mouse Ki-67 (Dianova, Hamburg, Germany), rabbit anti-laminin (Dako, Glostrup, Denmark), rabbit anti-GFP (a kind gift of Huib Croes, Department of Cell Biology, Radboud University Nijmegen Medical Center, The Netherlands), and mouse anti-thrombospondin (Abcam Limited) antibodies.

To examine metastatic deposits in lungs of mice carrying subcutaneous tumors, lungs were cut in five to six slices and arranged in tissue blocks in such a way that in one section a representative overview through the lungs is obtained. Numbers of metastases were counted in H&E stained sections. Differences in metastatic load between tumor groups were studied using Mann-Whitney *U*-test. Statistics were performed using SPSS software (SPSS Inc, Chicago, IL).

### Cell Lines and Transfections

Mel57 human melanoma cells were cultured in Dulbecco's modified Eagles' medium (Cambrex Bioscience, Verviers, Belgium) supplemented with 10% fetal calf serum (Cambrex), 100 U/ml penicillin, and 100  $\mu$ g/ml streptomycin (Cambrex) at 37°C at 5% CO<sub>2</sub>. cDNA encoding vascular endothelial growth factor (VEGF)-A<sub>165</sub> (human origin) was cloned in pIREShyg essentially as described.<sup>25</sup> Human Sema3E cDNA was obtained by reverse transcription polymerase chain reaction (RT-PCR) on glioblastoma RNA, using primers HpaI-Sema3E (5'-CGTTAA-CAGGGCTTGGACGG-3') and BstXI-Sema3E (5'-CCAG-CACACTGGTCAGGAGTCCAGCGT-3') and cloned in the EcoRV/BstXI sites of vector pIRESneo (Clontech, Palo Alto, CA) to generate plasmid pIRESneoSema3E. In parallel, Sema3C was PCR cloned in pIRESneo. Mel57 melanoma cells, stably transfected with pIREShyg-VEGF-A<sub>165</sub> were supertransfected with plasmid pIRESneoSema3E or

pIRESneoSema3C using Fugene reagent (Roche, Almere, The Netherlands). Two days after transfection, cells were put under hygromycin and neomycin selection pressure until colonies could be expanded. Similarly, double transfectants of Mel57 were generated expressing VEGF-A<sub>165</sub> and enhanced green fluorescent protein (EGFP) as control. The presence of recombinant VEGF-A, Sema3E, and Sema3C in conditioned medium was confirmed by Western blot analysis using VEGF-A20 antibody (Santa Cruz Biotechnology, Santa Cruz, CA), goat anti-Sema3E antibody (Abcam Limited), and sheep anti-Sema3C antibody (R&D Systems, Oxon, UK) respectively.

### Animals

All animal experiments were approved by the Animal Experiment Committee of the Radboud University. Specific pathogen-free, male BALB/c nude mice, 6 to 8 weeks of age were housed under specific pathogen-free conditions (five mice/cage, temperature 20°C to 24°C; relative humidity 50% to 60%; 15 air changes per hour; light-dark periods 14 hours/10 hours). Water and food (RMH, Hope Farms, The Netherlands) were available to the animals *ad libitum*.

### Metastasis Model

Groups of mice were injected subcutaneously in the flank with  $2 \times 10^6$  Mel57-VEGF-A/Sema3E cells ( $n = 9$ ), Mel57-VEGF-A/Sema3C cells ( $n = 9$ ), or Mel57-VEGF-A/EGFP cells ( $n = 8$ ) in 200  $\mu$ l PBS, essentially as described.<sup>26</sup> To be able to analyze mono- or multicellular origin of metastases, we tagged the tumors by co-injecting  $4 \times 10^5$  Mel57-EGFP cells. Tumor growth was monitored twice weekly and volumes calculated as height  $\times$  depth  $\times$  width. Mice were sacrificed after development of severe cachexia owing to tumor load, which was 28 and 37 days post subcutaneous injection of Mel57-VEGF-A/EGFP and Mel57-VEGF-A/Sema3(C/E) cells respectively. One out of nine animals carrying a Mel57-VEGF-A/Sema3E tumor had to be sacrificed 2 days earlier because of severe ascites and tumor deposits on the peritoneum. Before sacrifice, blood plasma was collected for determination of circulating VEGF-A levels by an in-house developed enzyme-linked immunosorbent assay.<sup>27</sup>

### Expression of Extracellular Matrix and Adhesion Molecules

Total RNA was isolated from 30 frozen 20- $\mu$ m sections of subcutaneous Mel57-VEGF-A ( $n = 5$ ) and Mel57-VEGF-A/Sema3E ( $n = 5$ ) tumors using TRIzol reagent (Invitrogen, Carlsbad, CA) according to the manufacturer's protocol and treated with DNaseI (NEB, Ipswich, MA). RNA samples (1  $\mu$ g) were reverse transcribed using MMLV reverse transcriptase (Promega, Leiden, The Netherlands) according to the manufacturer's instructions. In each individual sample, cDNA quality was assessed by PCR for

$\beta$ -actin and VEGF-A. Of each tumor group, cDNAs were pooled and subjected to the human extracellular matrix and adhesion molecules RT<sup>2</sup> profiler array (Superarray Bioscience Corporation, Frederick, MD). Amplification was performed in a volume of 25  $\mu$ l containing 1  $\mu$ l of template cDNA, 12.5  $\mu$ l of RT<sup>2</sup> real-time SYBR Green/ROX PCR master mix, 10.5  $\mu$ l of H<sub>2</sub>O, and 1  $\mu$ l RT<sup>2</sup> primer set. Amplification was performed for 40 cycles (95°C for 15 seconds, 60°C for 1 minute) on an ABI 7000 Real-Time PCR System (Applied Biosystems, Foster City, CA). For data analysis the  $2^{-\Delta\Delta C_t}$  method<sup>28</sup> was used with normalization of raw data to the housekeeping gene glyceraldehyde-3-phosphate dehydrogenase. Fold change values are presented as difference in expression due to Sema3E-overexpression in Mel57-VEGF xenografts. Cut off values for significant up- or down-regulation were chosen as 3 and 0.3, respectively.

### Results

#### PLXND1 and Sema3E Expression in Human Melanocytic Lesions

##### (Dysplastic) Naevi

We analyzed PLXND1 and Sema3E expression in benign melanocytic lesions, primary melanomas of different stage, and melanoma metastases to determine whether this receptor/ligand couple could be involved in tumor progression. As shown by immunohistochemistry with single domain antibody A12, PLXND1 expression was absent in melanocytes in both naevocellular naevi and dysplastic naevi (Figure 1, A and B respectively). Furthermore, no vessel-associated PLXND1 expression was observed in naevi. In the majority of naevi, we observed immunoreactivity on cells that appeared to be subsets of macrophages (arrow in Figure 1A) as determined by CD68

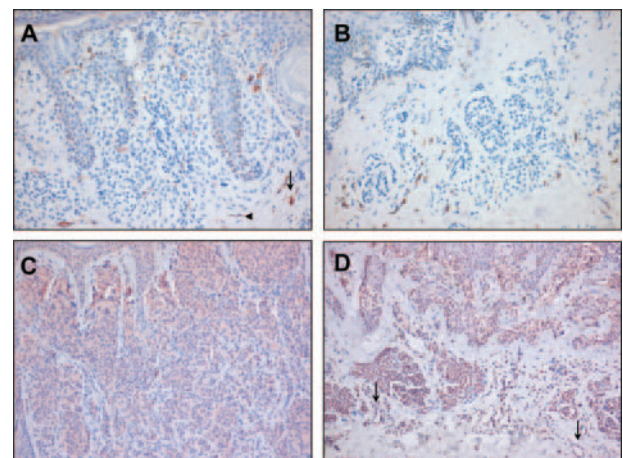


**Figure 1.** Immunohistochemical analysis of PLXND1 and Sema3E expression in naevi. PLXND1 is not detected in melanocytes in naevocellular (A) and dysplastic (B) naevi. Note the PLXND1-positivity of macrophage- (arrow in A) and fibroblast-like (arrowhead in A) cells. Melanocytes in naevocellular (C) and dysplastic (D) naevi abundantly express Sema3E. Note that vessels in a dysplastic naevus express Sema3E (arrows in D). Magnification = original  $\times 200$  (A, B) and  $\times 100$  (C, D).

**Table 1.** Membranous PLXND1 Expression in Melanocytic Cells in Benign Naevi, Primary Cutaneous Melanomas, and Melanoma Metastases

% Positive melanocytic cells	Naevi naevocellularis	Dysplastic naevi	Melanomas <i>in situ</i>	Primary melanomas			Melanoma metastases			
				Clark II	Clark III	Clark IV	Skin	Lymph node	Brain	Lung
0	19	10	5	4	2		1	1		
1–25					2					
26–50						2		1		
51–75				1		1				
76–99				2	1	1				
100					4		3	7	5	1
N <sup>+</sup> /N <sub>t</sub> <sup>*</sup>	0/19	0/10	0/5	3/7	3/5	10/10	3/4	8/9	5/5	1/1
%	0%	0%	0%	43%	60%	100%	75%	89%	100%	100%

\*Number of PLXND1 positive lesions (N<sup>+</sup>) per total number of examined lesions (N<sub>t</sub>).

staining (not shown) and fibroblast-like cells (arrowhead in Figure 1A). Whereas PLXND1 was not expressed by melanocytes, Sema3E was abundantly expressed in melanocytes, in approximately 80% and 75% of the naevocellular (Figure 1C) and dysplastic (Figure 1D) naevi, respectively. The vasculature in all but one dysplastic naevi also stained positive for Sema3E (arrows in Figure 1D).

### Primary Cutaneous Melanoma

Tumor cells in melanomas *in situ* were negative for PLXND1 (Table 1). However, 73% of the primary cutaneous melanomas exhibited membranous PLXND1 expression by tumor cells. The PLXND1 expression pattern varied per tissue sample from focal to homogeneous throughout the tumor. PLXND1 expression by tumor cells increased during progression from Clark II to IV (Table 1), with 43% of Clark II melanomas (Figure 2A) and 100% of Clark IV melanomas (Figure 2B) showing tumor cell-associated PLXND1 to some extent. Also within tumors, the

percentage of PLXND1-positive melanoma cells increased with Clark level (Table 1). In 40% of Clark IV primary cutaneous melanomas, all tumor cells expressed PLXND1 (Figure 2B). Whereas PLXND1 expression on tumor cells correlated with Clark level, we did not find a correlation between tumor cell PLXND1 expression and tumor thickness according to the Breslow index. However, vascular expression of PLXND1 did increase with tumor thickness. PLXND1-positive tumor vessels were absent in primary cutaneous melanoma thinner than 2 mm, while 83% of the lesions (Clark IV melanomas) thicker than 2 mm showed PLXND1-positive tumor vessels (Table 2). The arrows in Figure 2B point at PLXND1-positive tumor vessels in a Clark IV melanoma with a Breslow thickness of 3.2 mm. Even in a Clark IV melanoma with a Breslow thickness of 0.65 mm, tumor vessels were negative (arrow in Figure 2C).

The increase in PLXND1 expression was not paralleled by Sema3E expression, which was not significantly different between Clark II, III, and IV melanomas (Table 3). The inset in Figure 2B shows an example of a PLXND1-positive Clark IV melanoma in which no Sema3E expression is detected. Interestingly, blood vessels in Clark II (inset in Figure 2C) and Clark III melanomas stained positive for Sema3E, whereas in Clark IV lesions Sema3E-negative vessels were present too.

### Melanoma Metastases

Approximately 90% of the melanoma metastases showed PLXND1 immunoreactivity (Table 1). A homogeneous expression pattern on all melanoma cells was observed in 75% and 78% of the skin and lymph node metastases respectively, while only one lymph node metastasis showed focal PLXND1 expression by tumor cells (not shown). Consistent with our earlier observations, PLXND1 was abundantly expressed by both melanoma

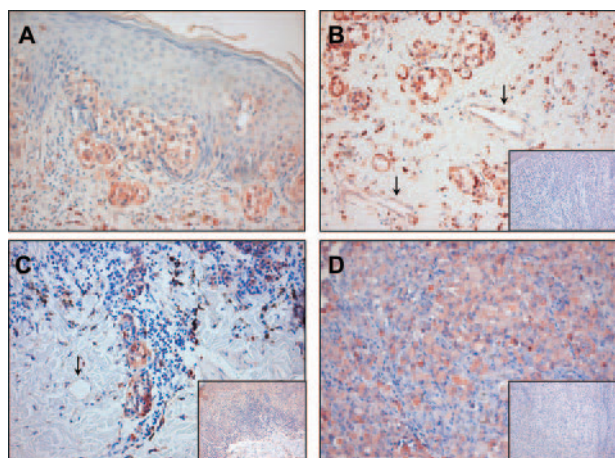


**Figure 2.** PLXND1 expression in primary melanomas and a melanoma metastasis as revealed by immunostaining with single domain antibody A12. Shown are PLXND1 positive tumor cells in a Clark II melanoma (A), Clark IV melanomas (B and C) and a lymph node metastasis (D). Note in B that tumor vessels in a melanoma with a Breslow thickness of 3.2 mm express PLXND1 (arrows), while PLXND1 is absent in the vasculature of a Clark IV melanoma with a Breslow thickness of 0.65 mm (arrow in C). The insets in B, C and D show Sema3E staining in a Clark IV melanoma (B), a Clark II melanoma (C), and a lymph node metastasis (D). Magnification = original  $\times 200$  (A–D) and  $\times 100$  (insets).

**Table 2.** PLXND1 Expression in Clark IV Melanomas

	Breslow thickness	
	<2 mm	$\geq 2$ mm
Melanoma cells	4	6
Tumor vasculature	0	5

**Table 3.** Sema3E Expression in Melanocytic Cells in Benign Naevi, Primary Cutaneous Melanomas, and Melanoma Metastases

% Positive melanocytic cells	Naevi naevocellularis	Dysplastic naevi	Melanomas <i>in situ</i>	Primary melanomas			Melanoma metastases		
				Clark II	Clark III	Clark IV	Skin	Lymph node	Brain
0	2	1		1	1	1	2	5	2
1-25				1		2	2	1	
26-50						1		1	1
51-75									
76-99	1			1					
100	8	3	4	3	3	3			
N <sup>+</sup> /N <sub>t</sub> <sup>*</sup>	9/11	3/4	4/4	5/6	3/4	6/7	2/4	2/7	1/3
%	82%	75%	100%	83%	75%	86%	50%	29%	33%

\*Number of Sema3E positive lesions (N<sup>+</sup>) per total number of examined lesions (N<sub>t</sub>).

cells and tumor vessels in brain and lung metastases. In contrast, both the number of melanoma metastases expressing Sema3E and the percentage of Sema3E-positive melanoma cells in individual lesions were reduced compared to primary cutaneous melanomas (Table 3). Only 36% of the melanoma metastases in our series exhibited tumor cell expression of Sema3E, which furthermore was restricted to only a small number of melanoma cells in 60% of these metastases. In 64% of the melanoma metastases, blood vessels were negative for Sema3E whereas in the remaining 36%, Sema3E was expressed in less than 25% of the tumor vessels.

### *Sema3E Inhibits VEGF-A-Induced Micronodular Growth in Subcutaneous Angiogenic Melanoma Xenografts*

The unexpected inverse correlation between PLXND1 expression and its ligand Sema3E in melanoma progression series prompted us to examine whether expression of Sema3E functionally affects tumor development and metastatic behavior of VEGF-A-expressing subcutaneous Mel57 melanoma xenografts.<sup>26</sup> In these xenografts, tumor cells stain positive with our anti-PLXND1 single domain antibody (Figure 3A). In addition, we analyzed the effects of expression of Sema3C, the Neuropilin-1 dependent PLXND1 ligand, on tumor development and metastasis of these subcutaneous xenografts. Mel57-VEGF-A/Sema3E and Mel57-VEGF-A/Sema3C xenografts showed similar growth rates and developed somewhat delayed as compared to control Mel57-VEGF-A/EGFP xenografts (Figure 3B). Mice were sacrificed when tumors had reached comparable sizes. All mice exhibited comparable elevated VEGF-A levels in their plasma (3 to 5 ng/ml) suggesting that effects on tumor growth, morphology, and metastatic phenotype were due to Sema3 expression and not to low VEGF-A production by the tumor cells. In addition, VEGF-A expression in the xenografts was confirmed by mRNA *in situ* hybridization (not shown). Sema3E and Sema3C expression was determined by immunostaining on Mel57-VEGF-A/Sema3E (inset in Figure 3C) and -/Sema3C (inset in Figure 3E) xenografts respectively.

Whereas VEGF-A expressing Mel57 xenografts grew with a characteristic micronodular phenotype,<sup>26</sup> the ar-

chitecture of these tumors was remarkably different when Sema3E was co-expressed (Figure 3C). Mel57-VEGF-A/Sema3E xenografts consisted of a well vascularized rim of viable tumor cells (Figure 3D), while centrally these tumors were sparsely vascularized with numerous necrotic areas. This phenotype was not observed when Sema3C instead of Sema3E was co-expressed (Figure 3,

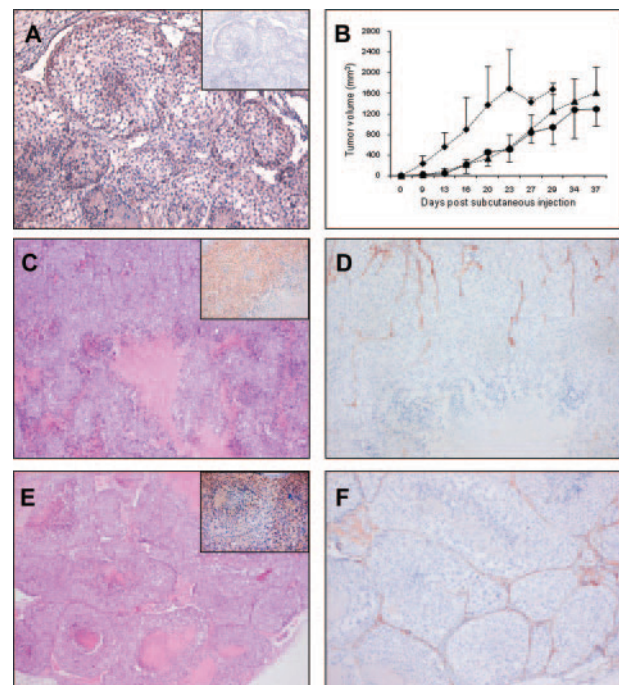


**Figure 3.** Analysis of subcutaneous Mel57-VEGF-A xenografts co-expressing Sema3E or Sema3C. **A:** PLXND1 expression in subcutaneous Mel57-VEGF-A xenografts as revealed by immunohistochemistry using single domain antibody A12. Both Mel57-VEGF-A cells and endothelium express PLXND1 (the inset shows a negative control staining with anti-VSV-G antibody). **B:** Tumor growth curves of Sema3E (●) and Sema3C(▲)-expressing Mel57-VEGF-A xenografts and control Mel57-VEGF-A/EGFP lesions (◆). Tumor volumes are calculated as height × depth × width. Note that the xenografts co-expressing Sema3(C/E) show comparable growth rates. Histological analysis of subcutaneous Mel57-VEGF-A/Sema3E and -/Sema3C tumors by H&E staining (**C** and **E**) and anti-CD34 staining (**D** and **F**). Note the absence of micronodular transformation in Sema3E-expressing tumors (**C** and **D**), while Mel57-VEGF-A/Sema3C xenografts show the typically VEGF-A induced micronodular growth pattern (**E** and **F**). In contrast to Mel57-VEGF-A/Sema3C xenografts, Sema3E-expressing tumors only show a well vascularized tumor rim. The insets in **C** and **E** show Sema3E and Sema3C immunostainings on Mel57-VEGF-A/Sema3E (**C**) and -/Sema3C (**E**) xenografts respectively. Magnification = original ×100 (**A**, insets), ×25 (**C**, **E**) and ×50 (**D**, **F**).

E and F). Staining for the proliferation marker Ki-67 with mouse Ki-67-specific antibodies revealed that, although *Sema3E* reduced tumor angiogenesis, VEGF-A-induced proliferation of vascular cells in the tumor rim was unaffected in Mel57-VEGF-A xenografts co-expressing *Sema3E* (not shown).

### *Sema3E* Reduces Metastatic Potential of Subcutaneous Mel57-VEGF-A Xenografts

We previously established that Mel57-VEGF-A tumors metastasize by shedding multicellular tumor fragments, surrounded by vessel wall elements, into the circulation, which eventually grow to large lung tumors, initially in pulmonary arteries.<sup>26</sup> The multicellular origin of these metastases was assessed by tagging tumor xenografts with EGFP-expressing tumor cells. This principle was also applied in the current experiments.

To investigate whether *Sema3E* affects metastatic capacity of Mel57 xenografts, we analyzed metastatic burden, composition, and localization of lung lesions. In mice carrying subcutaneous Mel57-VEGF-A/*Sema3E* xenografts, metastatic load in the pulmonary vessels was significantly reduced compared to Mel57-VEGF-A/EGFP ( $P = 0.022$ ) and -/*Sema3C* tumors ( $P = 0.006$ ) (Figure 4A). Whereas Mel57-VEGF-A/*Sema3C* xenografts exhibited the typical metastatic features previously described for Mel57-VEGF-A tumors<sup>26</sup> (Figure 4B), such phenotype was observed in only one mouse carrying a Mel57-VEGF-A/*Sema3E* xenograft. In two mice of the *Sema3E* group, small lung lesions in the tip of the lungs were detected (Figure 4C), which in contrast to lung metastases derived from Mel57-VEGF-A/*Sema3C* xenografts, lacked coverage by the vessel wall elements laminin (not shown) and endothelial cells (inset in Figure 4C).

Because we co-injected EGFP-tagged Mel57 cells, we could judge whether metastases were of multicellular or monoclonal origin. EGFP immunostaining revealed that the composition of most lung lesions derived from Mel57-VEGF-A/*Sema3C* xenografts was polyclonal with both Mel57-VEGF-A/*Sema3C* and Mel57-EGFP cells (Figure 4D), whereas the two Mel57-VEGF-A/*Sema3E* derived lesions located in the lung tip were composed of EGFP negative tumor cells (Figure 4E), suggesting that these originated from clonal expansion of single tumor cells rather than tumor emboli.

### *Subcutaneous Mel57-VEGF-A/Sema3E* Xenografts Display Down-Regulated Expression of Thrombospondin 1 and Extracellular Matrix Protein 1

Both angiogenesis and metastasis highly depend on extracellular matrix remodeling and establishing and disrupting cell-cell interactions. We therefore compared expression profiles of a number of extracellular matrix and adhesion molecules in Mel57-VEGF-A and Mel57-VEGF-A/*Sema3E* tumors using the Superarray RT<sup>2</sup> profiler kit. De-

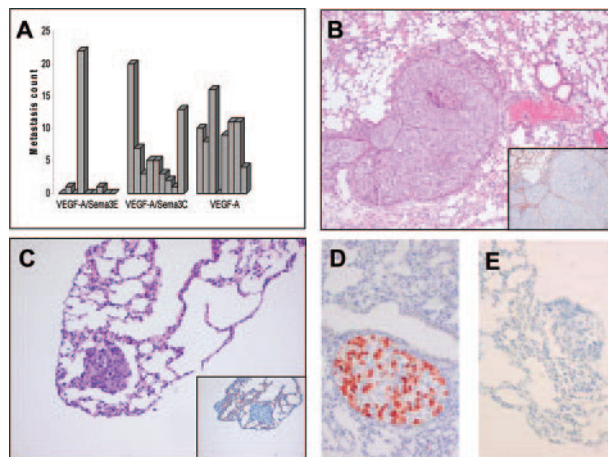


**Figure 4.** Analysis of metastatic burden, localization and composition. **A:** Metastatic count of mice carrying different subcutaneous Mel57-VEGF-A xenografts. Lung lesions were counted after H&E staining. Note that in mice carrying subcutaneous Mel57-VEGF-A/*Sema3E* xenografts metastatic burden is significantly reduced compared to Mel57-VEGF-A/EGFP ( $P = 0.022$ ) and -/*Sema3C* tumors ( $P = 0.006$ ). In contrast, metastatic load in mice carrying *Sema3C* expressing tumors is not significantly different from Mel57-VEGF-A/EGFP xenografts ( $P = 0.289$ ). Histochemical analysis of lung metastases by H&E staining (**B** and **C**) and anti-CD34 staining (insets) show that lung metastases derived from Mel57-VEGF-A/*Sema3C* xenografts (**B**) are predominantly located in the larger branches of the pulmonary vessels. Note in **C** that the small lesion in the tip of the lung derived from a Mel57-VEGF-A/*Sema3E* tumor is not surrounded by endothelial cells (inset in **C**). EGFP immunostaining on lung metastases derived from Mel57-VEGF-A/*Sema3C* (**D**) and -/*Sema3E* (**E**) xenografts tagged with EGFP-expressing tumor cells. Note that most lung metastases derived from Mel57-VEGF-A/*Sema3C* xenografts are of multicellular origin with both Mel57-VEGF-A/*Sema3C* and Mel57-EGFP cells (**D**), while the EGFP-negative lung lesion in mice carrying a subcutaneous Mel57-VEGF-A/*Sema3E* xenograft likely originates from clonal expansion of a single tumor cell (**E**). Magnification = original  $\times 50$  (**B**) and  $\times 100$  (**C**, **D**, **E**, insets).

tectable PCR products, defined as requiring  $<30$  cycles, were obtained for 41 out of 83 genes analyzed.

Neither of the tested genes were significantly up-regulated in tumors expressing *Sema3E* as compared to Mel57-VEGF-A tumors. However, we found that thrombospondin 1 (THBS1) and extracellular matrix protein 1 (ECM1) were expressed at significantly lower levels (respectively 3.8- and 3.6-fold lower as compared to Mel57-VEGF-A xenografts, Figure 5A).

To validate the RT-PCR array results we examined THBS expression at the protein level using immunohistochemistry on frozen sections of Mel57-VEGF-A and Mel57-VEGF-A/*Sema3E* tumors. In accordance with our array data, these immunostainings revealed that THBS is abundantly expressed in Mel57-VEGF-A xenografts (Figure 5B), but hardly detectable in Mel57-VEGF-A/*Sema3E* tumors (Figure 5C). Note that our staining protocol, using a mouse monoclonal THBS antibody, inevitably also results in non-specific staining of mouse IgG in necrotic areas in both tumors (see negative control stainings with anti-mouse secondary antibody only, insets). Comparison with these control stainings clearly shows that THBS is associated with the network of vessel wall elements in Mel57-VEGF-A lesions. Importantly, in these xenografts THBS is expressed by Mel57-VEGF-A cells (magnification in B), while tumor cells overexpressing *Sema3E* lack THBS expression (magnification in C).

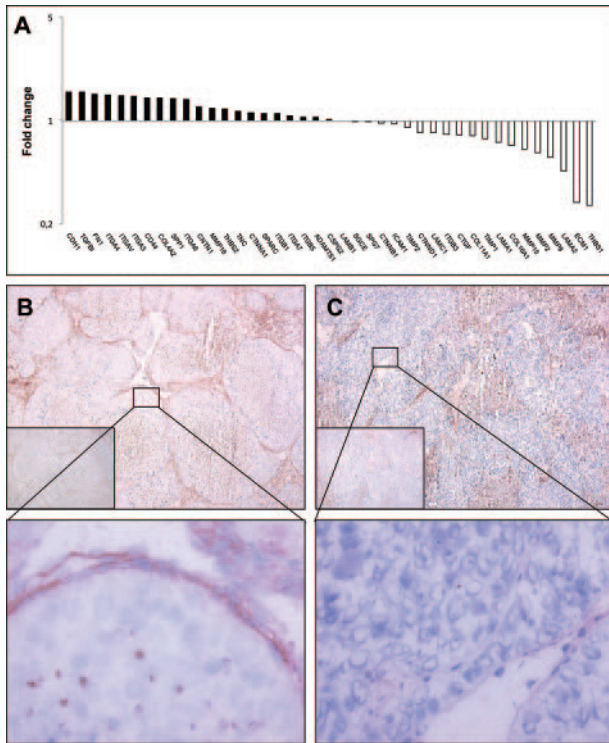


**Figure 5.** Fold-changes in mRNA expression of extracellular matrix and adhesion molecules in Sema3E overexpressing tumors relative to the control subcutaneous Mel57-VEGF-A lesions as revealed by RT-PCR array analysis (A). Columns represent fold changes in expression in Sema3E-expressing tumors relative to subcutaneous Mel57-VEGF-A lesions. Upper columns (>1.00) represent molecules whose mRNA expression is up-regulated, lower columns (<1.00) represent molecules whose expression is down-regulated. Immunohistochemical analysis of THBS expression in subcutaneous Mel57-VEGF-A (B) and Mel57-VEGF-A/Sema3E xenografts (C). In contrast to Mel57-VEGF-A/Sema3E lesions THBS is abundantly expressed in Mel57-VEGF-A tumors (the insets show negative control staining with anti-mouse antibody). Note in B that THBS expression is clearly associated with the network of vessel wall elements and tumor cells. Magnification = original  $\times 50$  (B, C, insets) and  $\times 400$  (enlargements).

## Discussion

Previous studies have suggested a functional role of PLXND1 in developmental angiogenesis.<sup>19,20</sup> In later stages of embryonic development, endothelial cells lose PLXND1 expression and expression is absent in adult endothelial cells.<sup>18</sup> We demonstrated that PLXND1 is re-expressed on vasculature during tumor-associated angiogenesis in both animal tumor models and a number of human brain tumors.<sup>21</sup> Here we show that PLXND1 is expressed by the tumor vasculature in primary melanomas thicker than 2 mm. Transition from micro- to deeply invasive melanoma is accompanied by angiogenesis<sup>3,4</sup> which augments vascular invasion of melanoma cells.<sup>29</sup> Thus, our findings confirm our previous observation that PLXND1 is expressed on angiogenic endothelium and not in quiescent vasculature.

PLXND1 was also abundantly expressed by tumor cells, including metastatic melanoma cells. The presence of consensus motifs for Rac-Rho signaling in the intracellular domain of PLXND1<sup>18</sup> is consistent with a possible regulatory role in cellular migration and, thus, tumor progression.

Here we show using a single domain antibody against the most amino terminal part of PLXND1 that expression of this protein in melanocytic lesions is indeed correlated with malignancy stage, being absent in benign lesions and ubiquitous in metastatic cancer. An inverse relationship was observed with Sema3E, one of the PLXND1 ligands, which was largely absent in metastatic lesions. The hypothesis that emerges from these data, that Sema3E expression is linked to decreased metastatic potential, could be validated in a functional melanoma metastasis assay.

The role of Sema3E in tumor biology has been matter of debate in the literature. Originally this protein was discovered via array-analyses as being correlated to metastatic mamma carcinoma.<sup>24</sup> In a follow-up study, Christensen et al showed by RT-PCR that Sema3E was expressed by 69% of human mamma carcinoma metastases and overexpression resulted in increased tumor growth in lungs.<sup>30</sup> It has to be realized however, that in these experiments tumor cells were injected directly in the circulation. The initial and possibly rate-limiting steps of metastasis, invasive growth in extracellular matrix, and entry into the vasculature were thus lacking in these experiments.

An inhibitory role of Sema3E for cell migration has also been described. Sema3E acts via PLXND1 to serve as a chemorepellant for endothelial cells<sup>22,23</sup> and inhibits neo-angiogenesis *in vivo*.<sup>22</sup> Sema4A, which binds to the same region of PLXND1 as Sema3E, suppresses VEGF-A-mediated angiogenesis by down-regulating Rac-GTP-dependent cytoskeletal rearrangement,<sup>22</sup> and it is conceivable that Sema3E has a similar mode of action. This notion is supported by our finding that Mel57 xenografts overexpressing Sema3E and VEGF-A display large areas of central necrosis, consistent with poor angiogenesis. Yet, in vasculature in vital parts of Mel57 VEGF-A/Sema3E xenografts proliferating endothelial cells were observed, indicating that VEGF-A was still able to activate VEGF receptors on endothelial cells. We previously showed that metastasis from Mel57-VEGF-A xenografts develop by bulging of tumor nodules into dilated vessels, a process that is accompanied by gradual coverage of these nodules by endothelial cells.<sup>26</sup> For this process, both endothelial proliferation and migration are indispensable. Our data are therefore consistent with a model in which lack of metastatic capacity is due to impaired migration of endothelial cells.

The dualistic chemorepellant/chemoattractant properties that are contained within Sema3E appear to be controlled by proteolytic processing, converting a repelling full length Sema3E into an inducer of invasiveness.<sup>30</sup> The antibody used in our current study recognizes both full length Sema3E and the p61 degradation product. The absence of any immunoreactivity in metastatic cancer cells thus places doubt on whether similar proteolytic mechanisms are relevant for regulating Sema3E activity in melanoma. It has recently been described that the presence or absence of neuropilin may also be an important factor, determining the guidance properties of the Sema3E/PLXND1 complex.<sup>31</sup> Interestingly, immunostainings on our melanoma progression series revealed that

membranous expression of neuropilin-1 was almost exclusively observed in melanoma metastases and to a much lesser extent in primary melanomas (not shown), ruling out an involvement for neuropilin-1 in regulating *Sema3E* activity.

To obtain more insight in the underlying mechanisms of angiogenesis and metastasis inhibition by *Sema3E*, we examined expression levels of a series of genes involved in extracellular matrix remodeling and cell adhesion. *THBS1* and *ECM1* were significantly down-regulated in *Sema3E* overexpressing xenografts. It must be noted that we examined gene expression in tumor xenografts consisting of a mix of tumor and stromal cells. Although we can therefore not determine to which cell types the differences in gene expression can be attributed, validation of the array results by immunohistochemistry revealed that *Sema3E* overexpression results in lack of *THBS* expression by *Mel57* cells. *THBS* is a secreted protein that interacts with different types of collagen<sup>32,33</sup> and laminin.<sup>33</sup> These matrix proteins are major components of the vascular network surrounding *Mel57-VEGF-A* tumor noduli,<sup>26</sup> which explains the localization of *THBS* in *Mel57-VEGF-A* xenografts. Thus, our observations are in agreement with a model in which *THBS* is secreted by *Mel57-VEGF-A* cells followed by retention by vessel wall elements generating a bioreservoir of *THBS*. It remains to be established which mechanisms underlie down-regulation of *THBS* by *Sema3E* on the cellular level.

The role of *THBS1* in tumor progression is controversial. Whereas this protein is generally presented as an angiogenesis inhibitor, it has also been reported that *THBS1* promotes melanoma invasiveness and metastasis via modulation of melanoma-matrix interactions (for review, see<sup>34</sup>). Interestingly, in clinical cutaneous melanomas, *THBS1* expression correlates with microvessel density, tumor thickness, and the presence of vascular invasion.<sup>35</sup> Our results are thus in agreement with a pro-angiogenic and pro-metastatic effects of *THBS1* in melanoma progression.

We also found *ECM1* to be down-regulated in *Sema3E* expressing *Mel57* tumors. Expression of *ECM1* is closely associated with early stages of angiogenesis during embryonic development and this protein has also been shown to be expressed by tumor cells.<sup>36,36,37</sup> Concordant with our results, *ECM1* expression is associated with metastatic behavior.<sup>37</sup>

Several other class 3 semaphorins and plexins have been found to affect tumor growth and invasion. Whereas *Sema3A*, *3B*, and *3F* are described to be functional inhibitors of tumorigenesis and involved in inhibition of tumor cell spread,<sup>38–40</sup> binding of *Sema4D* to its high affinity receptor plexin *B1* contributes to invasive tumor growth and metastasis via activation of *Met* and *Ron* receptors.<sup>41,42</sup> Although we showed here that *PLXND1* expression is correlated with tumor invasion and metastasis in melanoma progression series, we could not reveal which of its ligands functionally contributes to tumor progression and metastasis. Overexpression of *Sema3C*, one of the other *PLXND1* ligands, did not affect metastasis of *Mel57* xenografts. In addition, immunostainings on a number of human melanocytic lesions revealed that

*Sema3C* was equally expressed in both benign and malignant tissue samples (not shown). Taken together, based on our data we consider it unlikely that binding of *Sema3C* to a *Neuropilin-1/PLXND1* complex contributes to tumor progression.

The correlation between *PLXND1* expression and level of melanoma invasion makes this protein a potentially valuable diagnostic marker. *PLXND1* can aid to distinguish primary cutaneous melanomas from naevi with a sensitivity of 73%. The observation that *PLXND1* is expressed in both tumor vessels and tumor cells in melanoma metastases may also have therapeutic relevance since the protein may be used for simultaneous targeting of different tumor compartments of metastatic melanomas, ie, melanoma cells and the tumor vasculature.<sup>21</sup>

In conclusion, *PLXND1* expression correlates with malignancy grade in tumors but the ligand responsible for *PLXND1* activation still has to be identified. *Sema3E* expression inhibits angiogenesis and metastasis in melanoma, possibly via down-regulation of matrix-associated proteins such as thrombospondin 1 and extracellular matrix protein-1. It remains to be elucidated whether *Sema3E* exerts its effect by competitive inhibition of as yet unknown activating *PLXND1* ligands.

## Acknowledgment

We thank Geert Poelen for excellent technical assistance with the animal work.

## References

1. Elder DE: Pathology of melanoma. *Clin Cancer Res* 2006, 12:2308s–2311s
2. Guerry D, Synnestvedt M, Elder DE, Schultz D: Lessons from tumor progression: the invasive radial growth phase of melanoma is common, incapable of metastasis, and indolent. *J Invest Dermatol* 1993, 100:342S–345S
3. Barnhill RL, Fandrey K, Levy MA, Mihm MC, Jr., Hyman B: Angiogenesis and tumor progression of melanoma. Quantification of vascularity in melanocytic nevi and cutaneous malignant melanoma. *Lab Invest* 1992, 67:331–337
4. Erhard H, Rietveld FJ, van Altena MC, Brocker EB, Ruiter DJ, de Waal RM: Transition of horizontal to vertical growth phase melanoma is accompanied by induction of vascular endothelial growth factor expression and angiogenesis. *Melanoma Res* 1997, 7 Suppl 2:S19–S26
5. Clark WH, From L, Bernardino EA, Mihm MC: The histogenesis and biologic behavior of primary human malignant melanomas of the skin. *Cancer Res* 1969, 29:705–727
6. Ruiter DJ and Van Muijen GN: Markers of melanocytic tumour progression. *J Pathol* 1998, 186:340–342
7. Johnson JP: Cell adhesion molecules in the development and progression of malignant melanoma. *Cancer Metastasis Rev* 1999, 18:345–357
8. Alonso SR, Ortiz P, Pollan M, Perez-Gomez B, Sanchez L, Acuna MJ, Pajares R, Martinez-Tello FJ, Hortelano CM, Piris MA, Rodriguez-Peralto JL: Progression in cutaneous malignant melanoma is associated with distinct expression profiles: a tissue microarray-based study. *Am J Pathol* 2004, 164:193–203
9. Bosserhoff AK: Novel biomarkers in malignant melanoma. *Clin Chim Acta* 2006, 367:28–35
10. Tamagnone L, Artigiani S, Chen H, He Z, Ming GI, Song H, Chedotal A, Winberg ML, Goodman CS, Poo M, Tessier-Lavigne M, Comoglio PM: Plexins are a large family of receptors for transmembrane, se-



- creted, and GPI-anchored semaphorins in vertebrates. *Cell* 1999, 99:71–80
11. Gherardi E, Love CA, Esnouf RM, Jones EY: The sema domain. *Curr Opin Struct Biol* 2004, 14:669–678
  12. Rohm B, Ottemeyer A, Lohrum M, Puschel AW: Plexin/neuropilin complexes mediate repulsion by the axonal guidance signal semaphorin 3A. *Mech Dev* 2000, 93:95–104
  13. Nakamura F, Kalb RG, Strittmatter SM: Molecular basis of semaphorin-mediated axon guidance. *J Neurobiol* 2000, 44:219–229
  14. Fujisawa H: Discovery of semaphorin receptors, neuropilin and plexin, and their functions in neural development. *J Neurobiol* 2004, 59:24–33
  15. Takahashi T, Fournier A, Nakamura F, Wang LH, Murakami Y, Kalb RG, Fujisawa H, Strittmatter SM: Plexin-neuropilin-1 complexes form functional semaphorin-3A receptors. *Cell* 1999, 99:59–69
  16. Perala NM, Immonen T, Sariola H: The expression of plexins during mouse embryogenesis. *Gene Expr Patterns* 2005, 5:355–362
  17. Behar O, Golden JA, Mashimo H, Schoen FJ, Fishman MC: Semaphorin III is needed for normal patterning and growth of nerves, bones and heart. *Nature* 1996, 383:525–528
  18. van der Zwaag B, Hellemons AJ, Leenders WP, Burbach JP, Brunner HG, Padberg GW, Van Bokhoven H: PLEXIN-D1, a novel plexin family member, is expressed in vascular endothelium and the central nervous system during mouse embryogenesis. *Dev Dyn* 2002, 225:336–343
  19. Gitler AD, Lu MM, Epstein JA: PlexinD1 and semaphorin signaling are required in endothelial cells for cardiovascular development. *Dev Cell* 2004, 7:107–116
  20. Torres-Vazquez B, Gitler AD, Fraser SD, Berk JD, Van NP, Fishman MC, Childs S, Epstein JA, Weinstein BM: Semaphorin-plexin signaling guides patterning of the developing vasculature. *Dev Cell* 2004, 7:117–123
  21. Roodink I, Raats J, van der Zwaag B, Verrijp K, Kusters B, Van Bokhoven H, Linkels M, de Waal RM, Leenders WP: Plexin D1 expression is induced on tumor vasculature and tumor cells: a novel target for diagnosis and therapy? *Cancer Res* 2005, 65:8317–8323
  22. Toyofuku T, Yabuki M, Kamei J, Kamei M, Makino N, Kumanogoh A, Hori M: Semaphorin-4A, an activator for T-cell-mediated immunity, suppresses angiogenesis via Plexin-D1. *EMBO J* 2007, 26:1373–1384
  23. Gu C, Yoshida Y, Livet J, Reimert DV, Mann F, Merte J, Henderson CE, Jessell TM, Kolodkin AL, Ginty DD: Semaphorin 3E and plexin-D1 control vascular pattern independently of neuropilins. *Science* 2005, 307:265–268
  24. Christensen CR, Klingelhofer J, Tarabykina S, Hulgaard EF, Kramerov D, Lukanidin E: Transcription of a novel mouse semaphorin gene, M-semaH, correlates with the metastatic ability of mouse tumor cell lines. *Cancer Res* 1998, 58:1238–1244
  25. Kusters B, Leenders WP, Wesseling P, Smits D, Verrijp K, Ruiters DJ, Peters JP, Der Kogel AJ, de Waal RM: Vascular endothelial growth factor-A(165) induces progression of melanoma brain metastases without induction of sprouting angiogenesis. *Cancer Res* 2002, 62:341–345
  26. Kusters B, Kats G, Roodink I, Verrijp K, Wesseling P, Ruiters DJ, de Waal RM, Leenders WP: Micronodular transformation as a novel mechanism of VEGF-A-induced metastasis. *Oncogene* 2007, 26:5808–5815
  27. Span PN, Grebenchtchikov N, Geurts-Moespot J, Westphal JR, Lucassen AM, Sweep CG: EORTC Receptor and Biomarker Study Group Report: a sandwich enzyme-linked immunosorbent assay for vascular endothelial growth factor in blood and tumor tissue extracts. *Int J Biol Markers* 2000, 15:184–191
  28. Livak KJ, Schmittgen TD: Analysis of relative gene expression data using real-time quantitative PCR and the 2(-Delta Delta C(T)) method. *Methods* 2001, 25:402–408
  29. Kashani-Sabet M, Shaikh L, Miller JR, III, Nosrati M, Ferreira CM, Debs RJ, Sagebiel RW: NF-kappa B in the vascular progression of melanoma. *J Clin Oncol* 2004, 22:617–623
  30. Christensen C, Ambartsumian N, Gilestro G, Thomsen B, Comoglio P, Tamagnone L, Guldborg P, Lukanidin E: Proteolytic processing converts the repelling signal Sema3E into an inducer of invasive growth and lung metastasis. *Cancer Res* 2005, 65:6167–6177
  31. Chauvet S, Cohen S, Yoshida Y, Fekrane L, Livet J, Gayet O, Segu L, Buhot MC, Jessell TM, Henderson CE, Mann F: Gating of Sema3E/PlexinD1 signaling by neuropilin-1 switches axonal repulsion to attraction during brain development. *Neuron* 2007, 56:807–822
  32. Galvin NJ, Vance PM, Dixit VM, Fink B, Frazier WA: Interaction of human thrombospondin with types I-V collagen: direct binding and electron microscopy. *J Cell Biol* 1987, 104:1413–1422
  33. Aho S and Uitto J: Two-hybrid analysis reveals multiple direct interactions for thrombospondin 1. *Matrix Biol* 1998, 17:401–412
  34. Trotter MJ, Colwell R, Tron VA: Thrombospondin-1 and cutaneous melanoma. *J Cutan Med Surg* 2003, 7:136–141
  35. Straume O and Akslen LA: Expression of vascular endothelial growth factor, its receptors (FLT-1, KDR) and TSP-1 related to microvessel density and patient outcome in vertical growth phase melanomas. *Am J Pathol* 2001, 159:223–235
  36. Han Z, Ni J, Smits P, Underhill CB, Xie B, Chen Y, Liu N, Tylzanowski P, Parmelee D, Feng P, Ding I, Gao F, Gentz R, Huylebroeck D, Merregaert J, Zhang L: Extracellular matrix protein 1 (ECM1) has angiogenic properties and is expressed by breast tumor cells. *FASEB J* 2001, 15:988–994
  37. Wang L, Yu J, Ni J, Xu XM, Wang J, Ning H, Pei XF, Chen J, Yang S, Underhill CB, Liu L, Liekens J, Merregaert J, Zhang L: Extracellular matrix protein 1 (ECM1) is over-expressed in malignant epithelial tumors. *Cancer Lett* 2003, 200:57–67
  38. Neufeld G, Shraga-Heled N, Lange T, Guttmann-Raviv N, Herzog Y, Kessler O: Semaphorins in cancer. *Front Biosci* 2005, 10:751–760
  39. Xiang R, Davalos AR, Hensel CH, Zhou XJ, Tse C, Naylor SL: Semaphorin 3F gene from human 3p21.3 suppresses tumor formation in nude mice. *Cancer Res* 2002, 62:2637–2643
  40. Nasarre P, Constantin B, Rouhaud L, Harnois T, Raymond G, Drabkin HA, Bourmeyster N, Roche J: Semaphorin SEMA3F and VEGF have opposing effects on cell attachment and spreading. *Neoplasia* 2003, 5:83–92
  41. Giordano S, Corso S, Conrotto P, Artigiani S, Gilestro G, Barberis D, Tamagnone L, Comoglio PM: The semaphorin 4D receptor controls invasive growth by coupling with Met. *Nat Cell Biol* 2002, 4:720–724
  42. Conrotto P, Corso S, Gamberini S, Comoglio PM, Giordano S: Interplay between scatter factor receptors and B plexins controls invasive growth. *Oncogene* 2004, 23:5131–5137